# Numerical analysis on current and optical confinement of III-nitride vertical-cavity surface-emitting lasers

**Ying-Yu Lai,[1] Shen-Che Huang, [1] Tsung-Lin Ho, [1] Tien-Chang Lu,[1,*] and Shing-Chung Wang[1]**

[1]*Department of Photonics, National Chiao Tung University, Hsinchu 300, Taiwan*
[*]*timtclu@mail.nctu.edu.tw*

**Abstract:** We report on the numerical analysis of the electrical and optical properties of current-injected III-nitride based vertical-cavity surface-emitting lasers (VCSELs) with three types of current confinement schemes: the conventional planar-indium tin oxide (ITO) type, the AlN-buried type without ITO, and the hybrid type. The proposed hybrid structure, which combines an ITO layer and an intracavity AlN aperture, exhibits not only uniform current distribution but also enhanced lateral optical confinement. Thus, the hybrid type design shows remarkably better performance including lower threshold current and series resistance compared with the planar-ITO type and the AlN-buried type. Furthermore, the multi-transverse mode lasing behavior induced by strong index guiding of the AlN aperture is suppressed to single transverse mode operation by reducing the aperture size. Such design provides a powerful solution for the high performance III-N based VCSELs and is also viable by using current state of the art processing techniques.



**OCIS codes:** (140.2020) Diode lasers; (250.7260) Vertical cavity surface emitting lasers.

## References and links

1. S. Nakamura, M. Senoh, S. Nagahama, N. Iwasa, T. Yamada, T. Matsushita, Y. Sugimoto, and H. Kiyoku, "Room-temperature continuous-wave operation of InGaN multi-quantum-well-structure laser diodes with a long lifetime," Appl. Phys. Lett. **70**(7), 868–870 (1997).
2. S. Nakamura, "The roles of structural imperfections in InGaN-based blue light-emitting diodes and laser diodes," Science **281**(5379), 956–961 (1998).
3. S. Nakamura, M. Senoh, S. Nagahama, N. Iwasa, T. Yamada, T. Matsushita, Y. Sugimoto, and H. Kiyoku, "Room-temperature continuous-wave operation of InGaN multi-quantum-well-structure laser diodes," Appl. Phys. Lett. **69**(26), 4056–4058 (1996).
4. A. A. Bergh, "Blue laser diode (LD) and light emitting diode (LED) applications," Phys. Status Solidi A **201**(12), 2740–2754 (2004).
5. T. C. Lu, C. C. Kao, H. C. Kuo, G. S. Huang, and S. C. Wang, "CW lasing of current injection blue GaN-based vertical cavity surface emitting laser," Appl. Phys. Lett. **92**(14), 141102 (2008).
6. T. C. Lu, S. W. Chen, T. T. Wu, P. M. Tu, C. K. Chen, C. H. Chen, Z. Y. Li, H. C. Kuo, and S. C. Wang, "Continuous wave operation of current injected GaN vertical cavity surface emitting lasers at room temperature," Appl. Phys. Lett. **97**(7), 071114 (2010).
7. Y. Higuchi, K. Omae, H. Matsumura, and T. Mukai, "Room-temperature CW lasing of a GaN-based vertical-cavity surface-emitting laser by current injection," Appl. Phys. Express **1**, 121102 (2008).
8. K. Omae, Y. Higuchi, K. Nakagawa, H. Matsumura, and T. Mukai, "Improvement in lasing characteristics of GaN-based vertical-cavity surface-emitting lasers fabricated using a GaN substrate," Appl. Phys. Express **2**, 052101 (2009).
9. T. Onishi, O. Imafuji, K. Nagamatsu, M. Kawaguchi, K. Yamanaka, and S. Takigawa, "Continuous wave operation of GaN vertical cavity surface emitting lasers at room temperature," IEEE J. Quantum Electron. **48**(9), 1107–1112 (2012).
10. E. Hashemi, J. Gustavsson, J. Bengtsson, M. Stattin, G. Cosendey, N. Grandjean, and Å. Haglund, "Engineering the lateral optical guiding in Gallium Nitride-based vertical-cavity surface-emitting laser cavities to reach the lowest threshold gain," Jpn. J. Appl. Phys. **52**(8S), 08JG04 (2013).
11. B. S. Cheng, Y. L. Wu, T. C. Lu, C. H. Chiu, C. H. Chen, P. M. Tu, H. C. Kuo, S. C. Wang, and C. Y. Chang, "High Q microcavity light emitting diodes with buried AlN current apertures," Appl. Phys. Lett. **99**(4), 041101 (2011).

#203364 - $15.00 USD Received 18 Dec 2013; revised 25 Jan 2014; accepted 26 Jan 2014; published 16 Apr 2014

12. PICS3D (Photonic Integrated Circuit Simulator in 3D) by Crosslight Software, Inc., Burnaby, Canada, 2005.
13. G. R. Hadley, "Effective index model for vertical-cavity surface-emitting lasers," Opt. Lett. **20**(13), 1483–1485 (1995).
14. C. W. Tee, C. C. Tan, and S. F. Yu, "Design of antiresonant-reflecting optical waveguide-type vertical-cavity surface-emitting lasers using transfer matrix method," IEEE Photon. Technol. Lett. **15**(9), 1231–1233 (2003).
15. J. Bengtsson, J. Gustavsson, Å. Haglund, A. Larsson, A. Bachmann, K. Kashani-Shirazi, and M.-C. Amann, "Diffraction loss in long-wavelength buried tunnel junction VCSELs analyzed with a hybrid coupled-cavity transfer-matrix model," Opt. Express **16**(25), 20789–20802 (2008).
16. Y.-A. Chang, T.-S. Ko, J.-R. Chen, F.-I. Lai, C.-L. Yu, I.-T. Wu, H.-C. Kuo, Y.-K. Kuo, L.-W. Laih, L.-H. Laih, T.-C. Lu, and S.-C. Wang, "Carrier blocking effect on 850-nm InAlGaAs/AlGaAs vertical-cavity surface-emitting lasers," Semicond. Sci. Technol. **21**(10), 1488–1494 (2006).
17. J. Piprek, R. Farrell, S. DenBaars, and S. Nakamura, "Effects of built-In polarization on InGaN–GaN vertical-cavity surface-emitting lasers," IEEE Photon. Technol. Lett. **18**(1), 7–9 (2006).
18. J. R. Chen, S. C. Ling, H. M. Huang, P. Y. Su, T. S. Ko, T. C. Lu, H. C. Kuo, Y. K. Kuo, and S. C. Wang, "Numerical study on optical properties of InGaN multi-quantum-well laser diodes with polarization-matched AlInGaN barrier layers," Appl. Phys. B **95**(1), 145–153 (2009).

## 1. Introduction

Over past few decades, developments of III-nitride (III-N) semiconductors are rapidly increased due to their promising potential for practical light emitting diodes and laser diodes [1–3]. Among these aspects, III-N with wide-direct-bandgap characteristics are highly appreciated for providing full-color emission in the visible region, which is very important for many applications, such as lighting, optical storage, projectors, bio-sensing and so on [4]. So far, III-N based edge emitting lasers (EELs) have been realized and become commercialized for high density optical storage applications. But reports on another type of semiconductor lasers, vertical-cavity surface-emitting lasers (VCSELs) with several superior optical characteristics such as single longitudinal mode emission, low divergence angle, low threshold and two-dimensional array capability compared to the EELs, are still limited in the III-N system. To date, the continuous wave (CW) current injection of GaN-based VCSEL with hybrid mirrors and full dielectric mirrors are successfully demonstrated [5–9]. The key improvement for these devices to achieve room temperature operation is using a thin intra-cavity planar transparent conducting layer, ITO, to reduce the absorption loss but maintaining the current spreading ability within the current aperture. Despite the room temperature current injected GaN-based VCSELs have been successfully demonstrated in the planar-ITO type VCSEL structure, they still suffer from the non-uniform gain distribution, poor lateral optical confinement and the optical loss induced by the intracavity transparent current spreading layer and dielectric current aperture, resulting in a higher optical loss and threshold gain [10]. For aforementioned concerns, we had investigated a high quality current injection microcavity light emitter by inserting an intra-cavity AlN current aperture and removing the transparent current spreading layer to reduce the optical loss and to introduce a lateral current/optical mode confinement [11]. Although the issue of optical loss was reduced, the AlN-buried structure would come across with other electrical problems like the limited gain area, current crowding and severe leakage current over active regions to prevent the lasing action.

In this report, we theoretically analyzed both optical and electrical properties of aforementioned planar-ITO type and AlN-buried type cavity designs and also proposed a hybrid structure consisting of a thin ITO layer and a buried AlN current aperture for achieving a good current spreading ability and an additional lateral confinement of both current and optical modes. A three-dimensional model, which was simplified to a cylindrical symmetry two-dimensional scheme, was employed for numerically simulating the intra-cavity phenomena including the current spreading, gain distributions and the optical mode profiles.

## 2. Simulation models

Since the structure possesses the cylindrical symmetry, the simulation model could be simplified to the two-dimensional (2D) scheme for there has no structure difference along the azimuthal direction. Coordinates including the vertical direction $Z$ and the lateral direction $R$ are based on the original point (O), which lies on the sapphire surface. The commercial software Photonic Integrated Circuit Simulator in 3D (PICS3D) [12], which self-consistently

#203364 - $15.00 USD Received 18 Dec 2013; revised 25 Jan 2014; accepted 26 Jan 2014; published 16 Apr 2014

comprises the computation of semiconductor transport equations, the optical gain and mode, the quantum well band structure, was employed to model above mentioned VCSEL designs. The carrier transport model includes drift and diffusion of electrons and holes, built-in polarization, Fermi statistics and thermionic emission at hetero-interfaces, as well as spontaneous and defect-related Shockley-Read-Hall (SRH) recombination of carriers were used to determine the carrier transport phenomena. For the calculation of the quantum wells regime, Schrödinger and Poisson equations were solved iteratively to account for the quantum well deformation with different device bias. Stimulated emission of photons within the quantum well was calculated by a free carrier model including the wurtzite energy band structure. For the optical model, transfer matrix method was used to compute optical transmission and corresponding longitudinal modes between multi-layer gain medium and DBR stacks. For the spatial confined structures, a convenient effective index method (EIM) was employed to describe the transverse modes [13–15]. The carrier distribution, gain distribution, wave equation and the transfer matrix method were used to solve coupled wave equations. When the round trip gain equaled to one, the laser achieved the threshold condition. And the photon density or the output power was computed from the complex frequency obtained in the coupled wave equations. The detailed frame works of VCSEL modeling by PICS3D can be referred to previous works [16, 17] and the GaN-based material parameters, including spontaneous and piezoelectric polarization, can be found elsewhere [18]. Besides, all of simulations were based on the coordinate system shown in Fig. 2(a). To verify the correctness of simulation model and consistency with experimental results, we firstly simulated the recently reported GaN-based VCSEL structure, as shown in Fig. 1. The simulation parameters such as layer thickness were taken from the experimental results reported from Lu *et al.* [6]. The blue spheres in Fig. 1 were extracted data from *ref. 6* and the red dash line represented the simulation result. It's obviously that threshold current and slope efficiency of simulation fit well with measurement result which validates our simulation model.

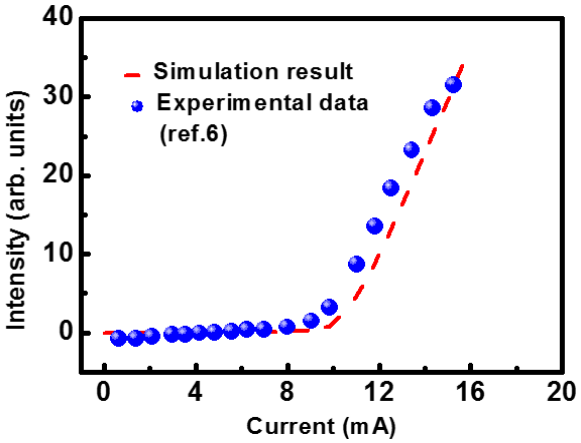


Fig. 1. Experimental (blue spheres) [6] and simulated output intensity of GaN VCSEL as a function of injection current.

### 3. Device structure

To systematically analyze the impacts of current confinement/spreading layers in the III-N VCSEL, we have taken into account three types of the VCSEL structures mentioned above. Figure 2(a) shows the proposed hybrid VCSEL structure with the transparent current spreading layer and the buried AlN current aperture. The structure has a 7λ thick cavity sandwiched by a bottom 29-pair AlN/GaN epitaxial distributed Bragg reflector (DBR) and a top 10-pair $Ta_2O_5/SiO_2$ dielectric DBR. The cavity composes of a 900 nm-thick n-GaN layer

#203364 - $15.00 USD Received 18 Dec 2013; revised 25 Jan 2014; accepted 26 Jan 2014; published 16 Apr 2014

(n-doping = 2.5 × $10^{18}$ $cm^{-3}$), 5 pairs $In_{0.2}Ga_{0.8}N$ (3 nm)/GaN (8 nm) multiple quantum wells (MQWs), a 20 nm-thick p-$Al_{0.12}Ga_{0.82}N$ (p-doping = 1 × $10^{18}$ $cm^{-3}$) electron blocking layer, a 100 nm-thick p-GaN (p-doping = 4 × $10^{17}$ $cm^{-3}$) layer, a 30 nm-thick AlN current aperture inserted into the p-GaN layer 90 nm up to the MQWs, and a 40 nm-thick ITO current spreading layer with the absorption loss less than 1%. For comparison, Fig. 2(b) to 2(d) display the enlarged p-side cavity structures of the planar-ITO, AlN-buried, and proposed hybrid type VCSELs, which would be used in the following simulation. It is worth noting that the VCSEL structures shown in Fig. 2(b) and Fig. 2(c) are similar to the previous reported devices [6], [11]. Figure 2(b) shows the planar-ITO VCSEL structure, for which the emitting aperture is defined by the $SiN_x$ passivation layer (radius of 5 μm). Our group has demonstrated lasing action by using this kind of current injection scheme [5], [6]. For the AlN-buried VCSEL structure, the current aperture is defined by the buried AlN layer with a smaller radius of 3.5 μm. Owing to the lack of ITO current spreading layer, a smaller current aperture is needed to achieve the laser action. Such device structure is similar to previously reported microcavity light emitting diodes (LEDs), which did not show lasing characteristics [11]. Figure 2(d) shows our proposed hybrid type structure, combining the ITO spreading layer and the AlN-buried aperture together, which current aperture is defined by AlN.

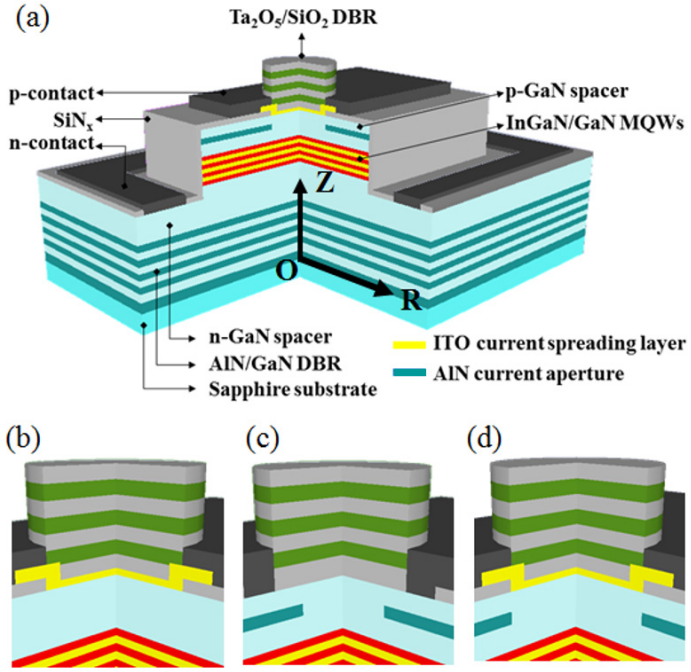


Fig. 2. (a) Schematic diagram of proposed ITO-AlN hybrid type GaN-based VCSEL. Z, R, O represent the vertical and lateral coordinate and the original point of simulation model, respectively. Enlarged structures of (b) planar-ITO, (c) AlN-buried, and (d) proposed hybrid type VCSEL. For the planar-ITO type VCSEL, the aperture is defined by the $SiN_x$; while the aperture is defined by the AlN for AlN-buried, and hybrid type VCSELs.

## 4. Simulation results and discussion

### *4.1 Current flow and gain distribution*

Since the simulation model was transferred to the 2D plane, the current flow should be divided into two directions: vertical (*Z*) and lateral (*R*). Figures 3(a)-3(c) and Figs. 3(d)-3(f) depict the vertical-flow and lateral-flow current density distributions in the MQWs around the aperture edges for the planar-ITO, AlN-buried, and hybrid type structures respectively.

#203364 - $15.00 USD Received 18 Dec 2013; revised 25 Jan 2014; accepted 26 Jan 2014; published 16 Apr 2014

Figures 3(a) and 3(d) depict a commonly seen current crowding issue in the planar-ITO case for those current densities flow along the vertical and lateral directions accumulated at the edge of the apertures. However, for the AlN-buried type, a more serious current crowding problem was observed in Figs. 3(b) and 3(e) due to the lack of current spreading layer and poor hole mobility of the p-GaN layer. The serious current crowding phenomena would induce the thermal accumulation and leakage current problems to limit the device performance. In our proposed hybrid type structure, the ITO layer and AlN current aperture maintained both the good current spreading and the current confinement capability, as shown in Figs. 3(c) and 3(f). The current densities were well confined inside the AlN aperture and were distributed more uniformly in the ITO-capping region compared to the AlN buried type structure without the ITO layer.

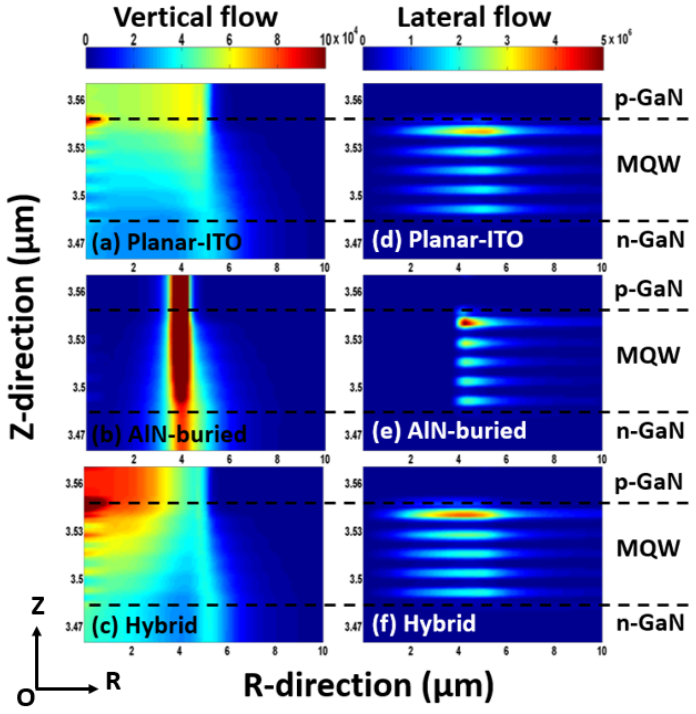


Fig. 3. Left column (a) to (c) and right column (d) to (f) represent the vertical-low and lateral-flow current density in the multiple quantum wells near the aperture edges of the planar-ITO, AlN-buried, and proposed hybrid type VCSEL, respectively. The figure coordinates axes are based on Fig. 2(a).

Figures 4 show the gain profiles of three types of VCSEL structures. In the planar-ITO structure, the aperture edge region had a higher gain compared to the central region due to the current crowding issue, as shown in Fig. 4(a). The maximum gain dispersed along the radial direction from the center of cavity would results in a poor spatial overlapping with the fundamental transverse cavity mode and a higher threshold. For the AlN-buried structure, a serious current crowding problem induced by the lack of the ITO current spreading layer resulted in a tiny gain area of the gain profile at the edge of the aperture and large optical loss in the center region of cavity, as shown in Fig. 4(b). Despite of the less absorption loss by removing the ITO layer, the poor overlapping between gain and fundamental optical mode and high loss in the central region could be the main reason preventing such device far away from lasing in the previous report [11]. As a consequence, we introduced the ITO spreading layer and buried AlN aperture in the proposed hybrid type structure for maintaining good current spreading and confinement capability. The larger contact area would enhance current

#203364 - $15.00 USD Received 18 Dec 2013; revised 25 Jan 2014; accepted 26 Jan 2014; published 16 Apr 2014

injection ability and mitigate the current crowding problem. So we could get a more uniform and broaden gain profile, as shown in Fig. 4(c). Such result would definitely provide a much better performance such as lower threshold current density and possibility of achieving single transverse mode operation.

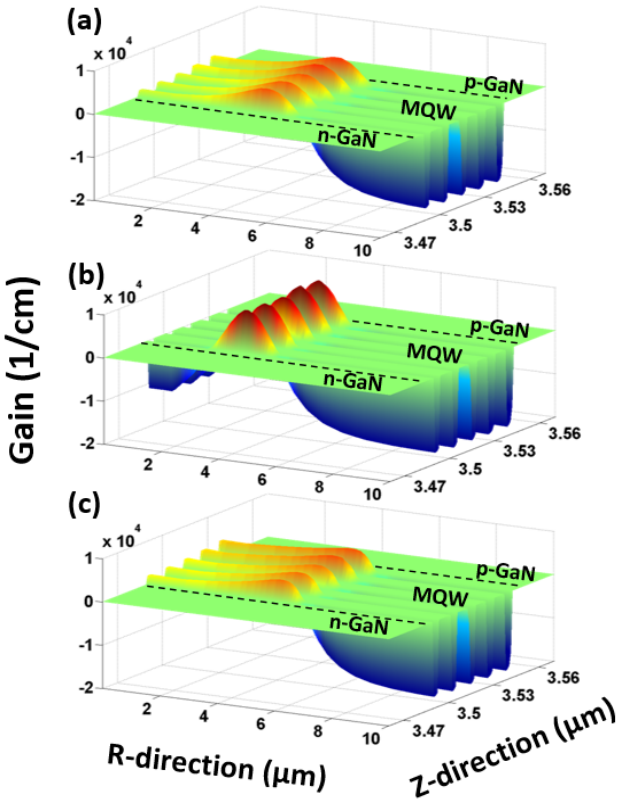


Fig. 4. Gain profiles in the multiple quantum wells near the aperture edges. (a) Planar-ITO (aperture radius 5μm): Slightly aggregation near aperture side, (b) AlN-buried (aperture radius 3.5μm): Gain gathers together in tiny area (c) proposed hybrid type (aperture radius 5μm): Uniform and broaden gain. The coordinates axis based on Fig. 2. The vertical axes represent the magnitude of gain (1/cm).

### *4.2 Optical mode guiding and gain-optical mode overlapping*

In addition to the electronic gain profile, another important role to affect the laser action is the overlapping percentage between the optical gain and cavity mode profile. In the vertical (longitudinal) direction (Z-direction), optical confinements achieved by highly reflective DBRs were almost the same in aforementioned three structures. Thus, the major factor to affect the threshold condition among these three structures would be the lateral (transverse) optical confinement (R-direction). It's noteworthy that AlN-buried type would not be discussed in the following since its laser action was limited by the edge accumulated gain distribution and high absorption loss at the central region from simulation results. In most of the simulation cases, the lasing threshold for the AlN-buried type device was significantly higher than other structure designs and would not be taken into analysis.

In the planar-ITO structure, the ITO layer was set at the node position of the optical field for reducing the absorption loss. But such approach resulted in negligible index difference and poor lateral optical confinement. Figure 5(a) depicts the optical mode and gain distribution within the QW which is most closed to p-GaN. As a result, planar-ITO case showed almost no optical guiding effect among different aperture sizes (only 0th mode appears), as shown in

#203364 - $15.00 USD Received 18 Dec 2013; revised 25 Jan 2014; accepted 26 Jan 2014; published 16 Apr 2014

Fig. 5(a). For the case with a smaller aperture size, the gain distribution showed more central-accumulated. The resulting gain-optical mode (0th) overlapping percentages for 3.5 μm, 4 μm, and 5 μm devices were 65.7%, 79.6%, and 83.6%, respectively. The smaller overlapping percentage resulted in a higher threshold current among smaller aperture device (shown in Fig. 5(b)).

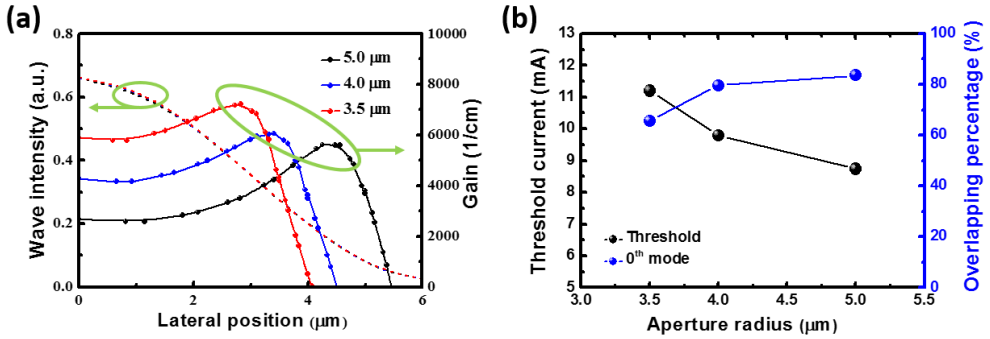


Fig. 5. Planar-ITO VCSEL case (a) Gain (solid line) and optical mode (dash line) distributions within the quantum wells along the lateral direction. Small aperture size makes the gain profile narrower and centralized but not the optical mode owing to the lack of lateral optical confinement. (b) Threshold and gain-optical mode overlapping percentage with different aperture radius. Threshold current increased with reducing aperture size due to poor overlapping between the gain and optical mode.

In order to solve the poor index guiding problem in the planar-ITO case, a low index AlN aperture was inserted in the *p*-GaN to provide effective index contrast for transverse optical mode guiding and a high resistance blocking layer for current confinement in the hybrid case. Such scheme could be regarded as a simple step-index circular waveguide and the ITO layer can still be kept. The transverse mode guiding ability could be verified using a normal EIM [13]. The effective index difference ($\Delta n_{eff} = n_{eff,cladding} - n_{eff,core}$) between p-GaN core region and AlN cladding can be easily calculated from the local resonance wavelength ($\Delta\lambda_0$) shift shown in the following equation:

$$\frac{\Delta n_{eff}}{n_{eff}} \approx \frac{\Delta\lambda_0}{\lambda_0} \tag{1}$$

Thanks to the buried AlN aperture, the hybrid type structure had better transverse confinement compared to the planar-ITO device with the same radius. The full width at half maximum (FWHM) of 0th order mode distribution in the lateral direction was narrowed from 3.5μm in the planar-ITO case to 3μm in the hybrid case. In such better optical confinement scheme, higher order modes may be evoked for the gain competition. To achieve single mode operation, the AlN aperture size should be reduced to enhance the overlapping between gain region and the 0th order fundamental mode. Figure 6(a) shows spatial distributions of the gain region (spheres with solid lines), 0th (short dash lines) and 1st (dash dot lines) order modes with different aperture size. From simulation results, device with 4.5 μm aperture radius had lowest threshold of 0th mode lasing due to its highest gain-optical mode overlapping with 0th mode and relatively smaller gain-optical mode overlapping for higher order mode (1th), as shown in Fig. 6(b). Figure 7 shows the L-I curves of 0th mode and 1st mode lasing. It's obviously that the lasing threshold of 1st mode decreased rapidly with larger aperture size due to good gain-optical mode overlapping. Furthermore, the increasing rates of 1st lasing mode output power become less rapidly in the 5 μm device at 35 mA and the 4.88 μm device at 40 mA representing the buildup of 2nd lasing mode. As the device radius reduced to 4.75 μm, the threshold current of 1st mode lasing significantly increased from 20 mA in 4.88 μm case to 42 mA, indicating, at this aperture size or an even smaller one, a wide single-transverse-mode operation range could be achieved when the injection current is even higher. It has to be

#203364 - $15.00 USD Received 18 Dec 2013; revised 25 Jan 2014; accepted 26 Jan 2014; published 16 Apr 2014

mentioned that 0th mode has a lower threshold with a smaller gain-optical mode overlapping compared with 1st mode is due to its lower diffraction loss. Such approach provides a very promising design for high performance GaN VCSELs.

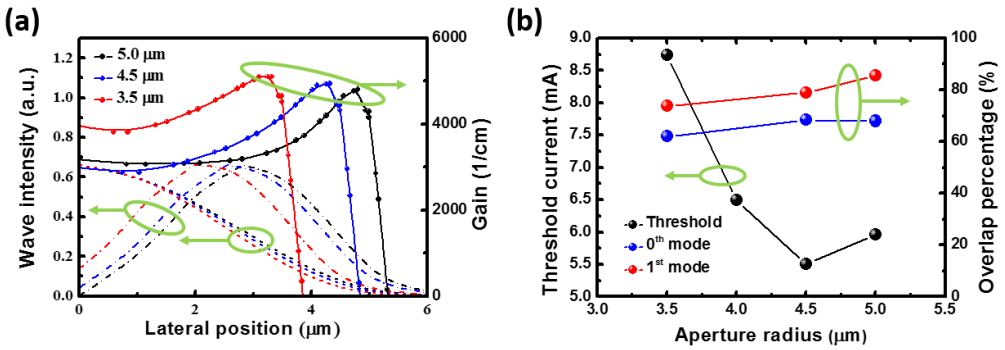


Fig. 6. (a) Gain (solid line), 0th (dash line), and 1st optical mode (dash-dot line) distributions within the quantum wells along the lateral direction. (b) Threshold (black dot) and gain-optical mode overlapping percentage of 0th (blue dot), and 1st optical (red dot) mode with different aperture radius.

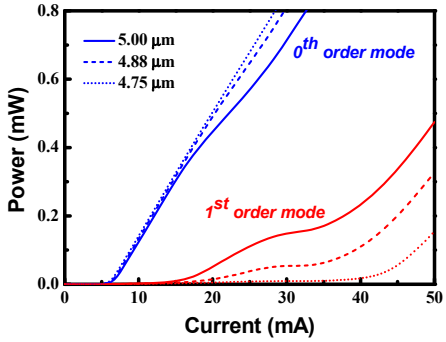


Fig. 7. L-I curves of 0th (blue line) and 1st (red line) mode lasing with different aperture radius (solid line for 5 μm, dash line for 4.88 μm, and dash line for 4.75 μm).

*4.3 Output power performance and voltage characteristics*

Figure 8 shows the light output power-current-voltage (L-I-V) curves of the planar-ITO, AlN-buried and proposed hybrid type VCSELs with apertures of 5 μm in radius. Due to the lack of the current spreading layer, the AlN-buried type device had the highest threshold among these three type structures due to the serious problem of current crowding, which may induce additional thermal and leakage effect. For the planar-ITO case, the absence of lateral optical confinement and injection difficulty of the small contact area defined by the $SiN_x$ aperture would limit the device performance including threshold current and turn-on voltage. With aforementioned consideration, the proposed hybrid type structure combined the advantages of better current spreading capability of the ITO layer and optical confinement of the buried AlN aperture. Besides, the lager contact area between ITO layer and *p*-GaN attributed to better current spreading and injection capability. According to these advantages, the hybrid type had the best performance. The threshold current could be reduced to even half of that of the planar-ITO type. The slope efficiency is also higher than the planar-ITO case. This may attribute to its better electrical confinement provided by the AlN aperture.

#203364 - $15.00 USD Received 18 Dec 2013; revised 25 Jan 2014; accepted 26 Jan 2014; published 16 Apr 2014

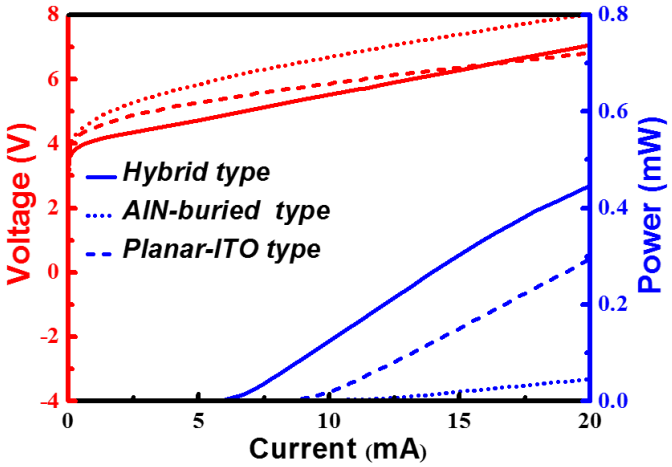


Fig. 8. The simulated light output power (blue line) and contact voltage (red line) characteristics of hybrid type (solid line), AlN-buried type (dot line), and planar-ITO type (dash line) VCSELs with apertures of 5 μm in radius as a function of injection current.

## 5. Conclusion

In summary, we have systematically analyzed the electrical and optical characteristics for the three types of VCSEL devices with different current spreading and optical confinement architectures and we have identified a better design for GaN-based VCSELs. The planar-ITO VCSEL suffered from the lack of lateral optical confinement and small contact area for current injection. The AlN-buried VCSEL exhibited a serious current crowding effect and longer current path which resulted in poor device performance. Our proposed hybrid type VCSEL not only provided better optical confinement but also retained good current injection. These advantages promised a better device design including low threshold current and turn-on voltage than previously reported structures. With further optimization of the AlN aperture position and opening structure such as the tapered shape and graded composition shall improve the GaN-based VCSEL performance. Such hybrid design could be used to realize high performance GaN-based VCSELs and even electrically driven polariton lasers for future scientific investigation.

## Acknowledgments

This work has been supported in part by the MOE ATU program and in part by the National Science Council of Republic of China (ROC) in Taiwan under Contract NSC 100-2628-E-009-013-MY3 and NSC 102-2221-E-009-156-MY3.